Tapia. Mariela ; Ramos, Leonard ; Heinemann, Detlev : Zondervan, Edwin

Power to the city: Assessing the rooftop solar photovoltaic potential in multiple cities of Ecuador

Journal Article	as:	published version (Version of Record)
DOI of this document*(secondary publication):		https://doi.org/10.26092/elib/2877
Publication date of this document:		20/03/2024

* for better findability or for reliable citation

Recommended Citation (primary publication/Version of Record) incl. DOI:

Tapia, Mariela, Ramos, Leonard, Heinemann, Detlev and Zondervan, Edwin. "Power to the city: Assessing the rooftop solar photovoltaic potential in multiple cities of Ecuador" Physical Sciences Reviews, vol. 8, no. 9, 2023, pp. 2285-2319. https://doi.org/10.1515/psr-2020-0061

Mariela Tapia*, Leonard Ramos, Detlev Heinemann and Edwin Zondervan

Power to the city: Assessing the rooftop solar photovoltaic potential in multiple cities of Ecuador

Abstract: Solar energy plays a crucial role in helping cities to decentralize energy production and thus decarbonize the energy mix. Reliable resource assessments are needed to support the deployment of solar power systems, especially in cities of developing countries where large solar potential remains untapped. The aim of this work is to assess the potential of rooftop solar photovoltaic (PV) in three populated cities in Ecuador's mainland (Quito, Guayaquil and Cuenca) and in the Galapagos Islands. The assessment involves (i) the estimation of the available rooftop area based on geographic information system data, (ii) the calculation of energy yield based on hourly satellite-derived irradiance and meteorological data, and (iii) the economic feasibility assessment in terms of levelized cost of electricity (LCOE) compared to representative electricity tariffs. In addition, a sensitivity analysis is carried out to assess the variability of the estimated technical and economic potential with respect to changes in the input parameters. The results reveal a total available rooftop area of about 144 km^2, mainly concentrated in urban parishes. The estimated energy yield is 16.94 ± 3.38 TWh/a, which could cover almost twice the annual energy consumption in 2019 of the study areas. The economic assessment shows that the LCOE ranges between 7.65 and 21.12 USD cents/kWh. However, the comparison of LCOE against representative residential tariff suggests that rooftop PV technology is not cost-competitive under most of the financial scenarios. The findings from this study will be of interest for local authorities and other decision makers to design policies and financing strategies to increase the penetration of rooftop PV and thus exploiting the large potential assessed in the study areas. The described methodology can be used for assessing the potential in other regions of Ecuador and thereby support the diversification and decarbonization of the energy mix in the country.

Keywords: Ecuador; geographic information systems; resource assessment; rooftop photovoltaic potential; urban solar potential.

***Corresponding author: Mariela Tapia**, Resilient Energy Systems Research Group, University of Bremen, Enrique-Schmidt-Str. 7, 28359, Bremen, Germany, E-mail: mariela.tapia@uni-bremen.de. https://orcid.org/0000-0003-3086-6078

Leonard Ramos and Detlev Heinemann, Energy Meteorology Group, Institute of Physics, University of Oldenburg, D-26111, Oldenburg, Germany

Edwin Zondervan, Laboratory of Process Systems Engineering, University of Twente, Horst – Meander, De Horst 2, 7522 LW, Enschede, Netherlands

https://doi.org/10.1515/psr-2020-0061

1 Introduction

Promoting renewables in cities could produce clean energy to meet urban energy demand and, at the same time, foster new businesses and create local job opportunities [1]. The use of solar photovoltaic (PV) systems installed on, or integrated with, the roofs and façades of buildings is increasing in cities of developed regions such as Europe and North America. This is driven not only by the flexibility and scalability of this technology, but also by its rapid development, which has reduced the cost of PV modules by more than 85% between 2009 and 2018 in most markets [2].

However, the deployment of PV systems in cities of development countries with higher solar potential is often at an earlier stage [1]. This is the case for Ecuador, a country located in the northwest of South America that has an important solar energy potential, since almost 55% of its territory shows solar radiation levels above 4.1 kWh m^{-2} d^{-1} [3]. However, in 2020, PV generation only accounted for 0.1% of the total electric power production, while the country continued relying on hydropower and fossil fuel thermal power (77.9% and 20.3%, respectively) for electricity generation [4]. Most of the installed solar capacity in Ecuador corresponds to ground-mounted PV farms. Nevertheless, since 2018 there is a new regulatory framework that supports the installation of PV systems up to 1 MWp (Megawatt peak) for self-consumption and also enables the injection of surplus energy into the grid under a monthly net energy balance scheme [5]. This has promoted the deployment of PV technology and by March 2021 there were 80 PV systems with a total capacity of 3.0 MWp for self-consumption of residential, commercial and industrial users [6].

To further promote the growth of PV systems installed on rooftops in Ecuadorian cities, reliable resource assessments are needed in order to understand the availability and variability of the solar resource on roof surfaces, as well as to evaluate the economic feasibility for implementing this technology in the country. Estimating the PV potential of an urban landscape is a complex task since building elevations, population densities, and different urban morphologies, combined with a lack of data, complicate the assessment [7]. The methodologies to assess the rooftop PV potential can be classified based on the data availability and the scale of the area under study into three categories: (i) sample methodology, (ii) multivariate sampling-based methodology and (iii) complete census methodology [7]. In the first category, sampling techniques are used to estimate the available roof surface which can then be extrapolated. Although these techniques are less accurate compared to the others, they are suitable for large regional assessments [8]. In the second category, multivariate sampling-based methodologies identify correlations between population density and available roof area by including additional variables to improve the accuracy. Considering that this methodology maintains a sample-based approach, the method is straightforward but, due to the inclusion of additional variables, it may be considered more time-consuming [7]. In the last category, the complete census methodologies are used to compute the

entire rooftop area of the study region either by processing statistical datasets of building-related information (e.g., floor area, number of floors, total number of buildings) or through digital cartographic datasets by applying Geographical Information Systems (GIS) data processing [7]. Geo-datasets of solar irradiance are also used to spatially analyze the available incident solar radiation [9]. Techniques in this category are generally expected to produce more accurate results, although, they can be considerably more time consuming and expensive compared to the previous two approaches [7].

Previous studies focused on Ecuador have assessed the potential of rooftop PV at a city level in Quito [10], Cuenca [11] and the Galapagos Islands [12]. Dávila and Vallejo [10] used an statistical approach to assess the technical and economic potential of PV rooftop for the 32 urban parishes of Quito. The available area for rooftop PV installation was calculated based on the characterization of the buildings surface area in two random blocks for each parish, which was then extrapolated to the entire urban area. The annual energy yield was calculated using average annual solar radiation values from one point inside each parish, which were retrieved from the typical meteorological year (TMY) dataset of the National Solar Radiation Database (NSRDB) [13]. The results showed that the estimated technical potential in the urban parishes of Quito was 557.1 GWh/a, while the economic potential could be 343.5 GWh/a, if the installed cost of PV systems decreases to 750 USD/kWp [10]. In the case of Cuenca, Barragán-Escandón et al. [11] used digital cadastral maps to calculate the available area of all roofs registered by the municipality up to 2015. Monthly averages of daily irradiation retrieved from the National Renewable Energy Laboratory (NREL) System Advisor Model (SAM) [14] were used to calculate the annual energy yield, assuming uniform irradiance over the study area. The results showed a theoretical potential of 1454.90 GWh/a, which could meet 3.19 times the electricity demand of the area. In the case of the Galapagos Islands, Tian et al. [12] calculated the annual rooftop PV system output for two urban settlements, namely Puerto Baquerizo Moreno and Puerto Ayora. Digital cadastral maps were used to estimate the total available rooftop area. The annual energy yield was calculated using the average annual solar radiation from the Global Solar Atlas [15]. Results showed that a minimum of 21% and 27% of the total rooftop area must be covered to meet the electricity demand in Puerto Baquerizo Moreno and Puerto Ayora, respectively [12].

The methods used in these studies can be fitted into the first and third categories mentioned above and have shown the great rooftop PV potential in these Ecuadorian regions. However, yearly or monthly aggregated irradiation values were used in the assessments without considering the spatial and temporal variability of the solar resource throughout the study area.

In this work, we present a GIS-based procedure to assess the rooftop solar PV potential time series using long-term hourly averages of gridded satellite-derived solar irradiance and thus taking into account the spatio-temporal variability of the solar resource. The assessment is performed for three densely populated cities in Ecuador's

mainland (Quito, Guayaquil and Cuenca) and the inhabited areas of the Galapagos Islands. The methodology used for this purpose involves the following stages (i) the estimation of the available rooftop area based on GIS data, (ii) the calculation of the energy yield based on satellite-derived irradiance and meteorological data through a PV system performance modeling toolbox in Python, and (iii) the economic feasibility assessment in terms of LCOE compared to representative electricity tariffs. In addition, a sensitivity analysis is carried out to assess the variability of the estimated technical and economic potential with respect to changes in the input parameters.

The remaining part of this work proceeds as follows. Section 2 describes the selected study areas. Section 3 describes the GIS and meteorological datasets used in the geospatial and technical assessments. Section 4 explains the methodology implemented in each stage of the assessment. Section 5 presents and discusses the results with a dedicated subsection for each stage of the assessment. Finally, Section 6 summarizes the main findings of this work.

2 Study area

Ecuador is located in the northwest of South America with a continental area located from 82 °W to 75 °W in longitude and from 5.1 °S to 1.5 °N in latitude, and the Galapagos Islands located between 91.7 °W and 89.2 °W in longitude and between 1.5 °S and 0.4 °N in latitude. The total surface area is 256,370 km^2, including the insular zone. The country is politically and administratively organized in regions, provinces, cantons and parishes (urban and rural) [16]. Currently, there are 24 provinces subdivided in 221 cantons [17].

This study is focused on three densely populated cities in Ecuador's mainland, specifically Quito, Guayaquil and Cuenca, which are located in the cantons with the same names. Additionally, the assessment also includes the Galapagos Islands, a natural protected area, where distributed renewable energy generation is a relevant topic since the islands are not connected to the mainland's power grid. Figure 1 shows the location of the selected study areas.

Quito is a metropolitan district that belongs to Pichincha province and is the country's capital. It is located in the northern Ecuadorian highlands, comprises 32 urban and 33 rural parishes and has a population of around 2.2 million inhabitants [19]. Guayaquil is the capital of Guayas province and the most populated canton with more than 2.3 million inhabitants [19], distributed in 16 urban and 5 rural parishes. It is located in the southwest Ecuador on the coastal area and is traditionally considered together with Quito as the poles of development [16]. Cuenca is the capital of Azuay province located in southern Ecuadorian highlands with a population of around 505 thousand inhabitants [19], distributed in 15 urban and 22 rural parishes. The Galapagos Islands comprise 13 major and six minor islands; though, only four of the major islands are inhabited, namely Santa Cruz, San Cristobal, Isabela and Floreana with a total population about 25 thousand [19].

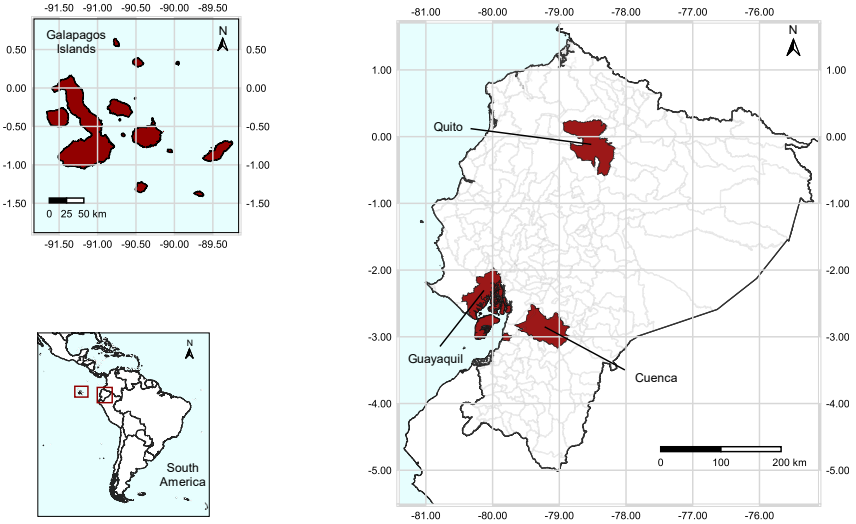

Figure 1: Location of the study areas in Ecuador's mainland and the Galapagos Islands. The continental area shows the administrative boundaries at canton level.
Source: Own representation, data retrieved from ref [18].

3 Data

3.1 GIS datasets

The calculation of the available rooftop area is based on publicly available GIS datasets mapping the human settlements of each study area, which were retrieved from the geoportal of the corresponding municipality (Table 1). Each dataset contains vector polygons representing (i) the building footprints of the urban and rural parishes of Quito and Cuenca (Figure 2a and c, respectively), (ii) the parcel lots of the urban and rural parishes of Guayaquil (Figure 2b), as well as the rural parishes of Cuenca (Figure 2c), and (iii) the urban zone boundaries of the four inhabited islands in Galapagos (Figure 2d).

In the case of parcel cadastral maps, where the vector polygons may contain buildings and ground area, a common approach to calculate the overall rooftop area is to apply a reduction factor that describes the relationship between gross ground floor area to rooftop area [7]. Thus, for the calculation of the roofed area in Guayaquil the maximum building coverage ratio of 65% established by the municipality [20] is used as the reduction factor. For Cuenca, we also use 65% as the reduction factor for the rural parishes, since the municipality does not set a specific maximum building coverage ratio, but rather defines it depending on the parcel area at 60% or 70% [21], therefore we use the midpoint for simplicity.

Table 1: Description of the GIS datasets used for the geospatial assessment.

Dataset	Type	Download date	Source
Digital cadastral map Quito	Building footprint	06.05.2021	[22]
Digital cadastral map Guayaquil	Cadastral parcels	06.05.2021	[23]
Digital cadastral map Cuenca	Building footprint and cadastral parcels	05.05.2021	[24]
Urban areas map Galapagos	Boundaries of urban zones	05.05.2021	[25]
Administrative boundaries map Ecuador	Digital map	20.04.2021	[18]

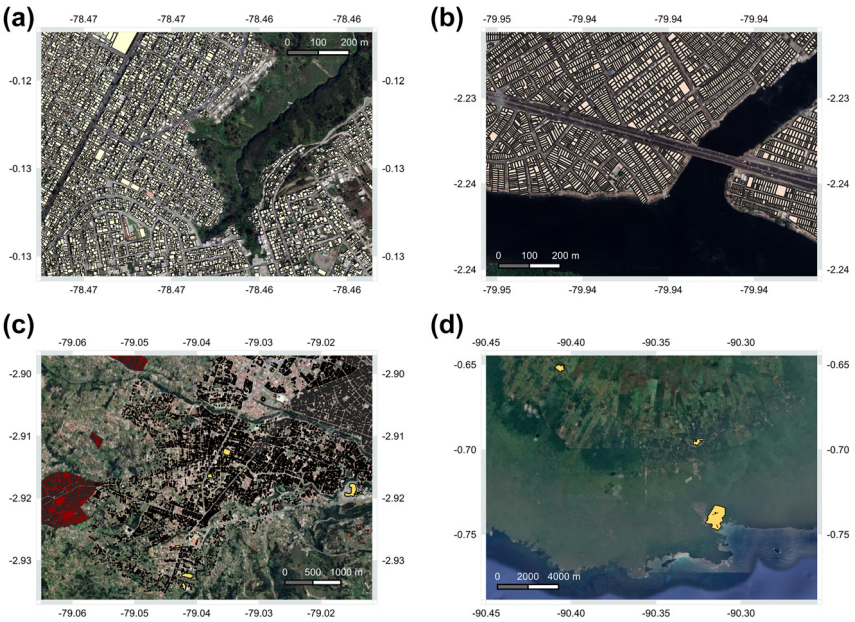

Figure 2: Partial captures of the GIS datasets (colored polygons) using Google satellite imagery as background.
(a) Building footprint of Quito, (b) cadastral parcels of Guayaquil, (c) building footprint of the urban parishes and cadastral parcels (red polygons) of the rural parishes in Cuenca, (d) urban zone boundaries of Santa Cruz Island in the Galapagos Island.
Source: Own representation, data retrieved from refs. [22–25].

A multiplication factor is also needed to calculate the roofed area of the inhabited areas of Galapagos based on the urban zone maps. To define this factor, we use as reference the findings of the assessment performed by Tian et al. [12], who had access to the digital cadastral maps of two parishes of Galapagos. According to their results,

Puerto Baquerizo Moreno (San Cristobal Island) and Puerto Ayora (Santa Cruz Island) have a total rooftop area of 0.324 km^2 and 0.392 km^2, respectively. These areas correspond to approximately 30% of the total urban zone area of each parish in the maps retrieved for our study. Thus, we use 30% as the reduction factor assuming similar characteristic in the four study islands.

3.2 Solar irradiance and meteorological data

The historical hourly time series from 1998 to 2018 of global horizontal irradiance (GHI), diffuse horizontal irradiance (DHI), direct normal irradiance (DNI) in [W/m^2], wind speed in [m/s] and ambient temperature in [°C] over Ecuador's mainland and the Galapagos Islands were retrieved from the NSRDB [13]. It should be noted that the spatial resolution of the dataset was increased from the native NSRDB resolution to 3×3 km by using the first order conservative remapping method. This post-processing was done to match the spatial resolution of various datasets we use in other studies (see more details in ref [26]).

To estimate the rooftop PV technical potential, we use the long-term hourly average dataset (i.e., 8760 time-steps for each grid point), which is calculated from the hourly irradiance and meteorological data over the period 1998–2018. This reduces the variability of the meteorological data and enables the estimation of the long-term PV potential without bias due to extreme events of a specific year [27].

4 Methodology

Figure 3 displays an overview of the methodology used in this study to estimate the rooftop PV potential. It comprises four different stages: (1) the geospatial assessment to calculate the available rooftop area using the GIS datasets, (2) the technical assessment to estimate the energy yield based on the gridded meteorological data and the resulting available rooftop area, (3) the economic assessment to evaluate the economic feasibility of PV technology in terms of LCOE under three financial scenarios, (4) the sensitivity analysis to quantify the variability of the annual energy yield and LCOE with respect to changes in the input parameters. Each of these stages is explained in more detail in the next subsections.

4.1 Geospatial assessment methodology

The geospatial assessment comprises the following steps, which are performed using QGIS 3.16 [28].

- ***Shapefile processing***: First, all digital cadastral and administrative boundaries maps are reprojected to the same coordinate reference system (World Geodetic System 1984, known as WGS84). Next, those polygons representing empty parcels are removed from the digital cadastral maps, because they can lead to overestimation of the rooftop area. Note that this removal is only possible for Guayaquil, since its GIS dataset contains information about the type of building in the attribute table.

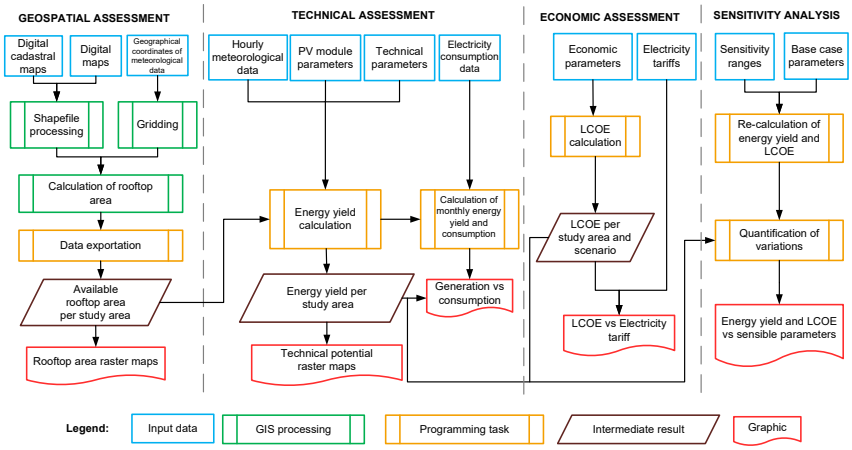

Figure 3: Overview of the applied methodology to estimate the rooftop PV potential.

- ***Gridding***: A process called "gridding" is carried out through an algorithm that creates a matrix of squares with a fixed area using a set of geographic coordinates as centroids. For this process, each administrative boundary map is divided into grid squares, whose centroids are the geographical coordinates of the gridded meteorological dataset. Each square has an area of 3×3 km^2. This procedure is necessary to ensure that both the subsequently calculated rooftop areas and the meteorological dataset match in terms of geospatial resolution, allowing the technical potential calculation afterwards. An illustration of this process over the digital map of Guayaquil is displayed in Figure 4a.
- ***Calculation of available rooftop area:*** Once the reference grid layer is built, the area of the polygons (which represent buildings from an aerial view) inside each grid square is calculated. This is performed using the geoprocessing tool of QGIS called "clipping" that overlays a vectorized layer with a vector boundary layer to extract the part inside the area of interest by eliminating areas outside of it [29]. In other words, only the polygons inside the boundary layer are extracted, resulting in a new subset of the original vector layer. The reference grid squares are used as the vector boundary and an iterative process is applied to extract those polygons inside each specific grid square (as illustrated in Figure 4b), and subsequently calculate their total area. This procedure is repeated for each grid square until the entire study area is covered. Then, a raster map is generated in which the calculated available rooftop area is associated with the corresponding geographical coordinates of the grid square centroid. At the end, this information is exported as comma-separated values (CSV) file to be used in the technical assessment stage.

4.2 Technical assessment methodology

4.2.1 Energy yield calculation: The pvlib-python package [30] is used to calculate the PV energy yield of the total available rooftop area of each grid square based on the hourly irradiance and meteorological dataset. The calculation requires a set of input parameters regarding the PV module specifications and the technical parameters of the PV system, namely (i) surface azimuth, (ii) tilt angle, (iii) the factor f_{loss} that accounts for capture and system losses, and (iv) the utilization factor f_{u} that is defined as the usable portion of the rooftop area for the installation of PV modules. The mono-crystalline silicon

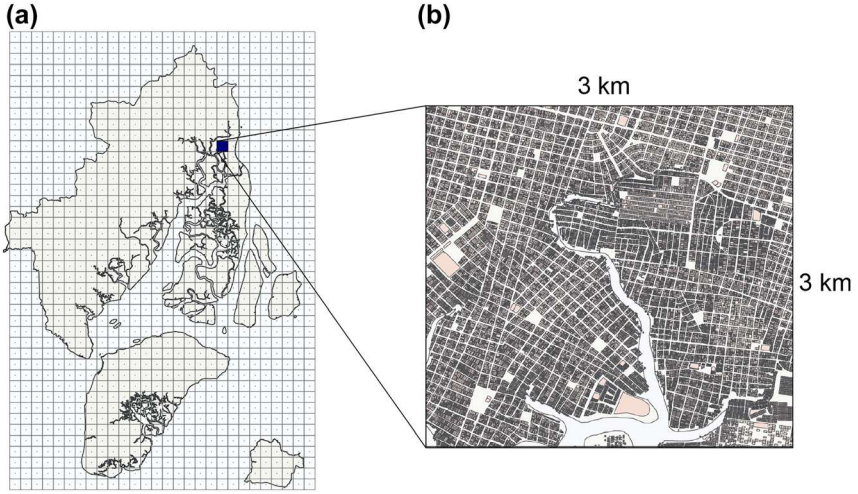

Figure 4: Illustration of the gridding process applied to Guayaquil's digital maps.
(a) Gridding generation over the digital map of administrative boundaries. (b) Clipping processing over the digital cadastral map.

module SPR 220 BLK-U from SunPower is used in the calculations (see specifications in Table A1 of Appendix A). The technical information of this module can be retrieved directly in pvlib-python.

For the base case calculations, the technical parameters of the PV system are defined as follows and are assumed to be uniform throughout the study areas. The surface azimuth is set at 0° respect to due north, since most of the territory of the study areas lays below the equator. The tilt angle is set at 20°, which is the midpoint of the typical inclination angle range (14° and 26°) of roofs in Cuenca found in ref. [31]. The factor f_{loss} is set at 14%, a typical value representing losses due to soiling, shading, mismatch, wiring, connections, light induced degradation, nameplate rating and operational availability [32], as well as cable and inverter losses [9]. Note that losses due to temperature are not included in f_{loss}, since pvlib-python uses a thermal model to predict the associated operating temperature of the PV modules based on the given meteorological dataset [33]. The utilization factor f_{u} is set at 50% based on ref. [34] that found that the average suitable area of residential buildings in the urban and rural area of Cuenca ranged between 49% and 51%.

After setting the base case technical parameters, the calculation of the energy yield is performed using the object-oriented modeling paradigm of pvlib-python [35]. The PV system object is instantiated with the selected PV module and the predefined tilt and azimuth angles. The Sandia Array Performance Model (SAPM) [33] is selected to model the electrical performance of the PV modules. The temperature of the PV modules and cells are modeled assuming a "close roof mount" mounting configuration [33], since we investigate the performance of PV systems installed on rooftops. The Hay-Davies model [36] is selected as the irradiance transposition model to get the plane of array (POA) irradiance components.

Then, an instance of the ModelChain class is created with the geographical coordinates of a grid point of location (s) and the previously defined PV system object. Next, the model is run with the hourly meteorological data of that grid point. In this step, the SAPM model simulates the characteristic current–voltage (I-V) curve that determines the output power of a single PV module under those specific meteorological conditions. The output is a time series that includes: short-circuit current (I_{sc}), open-circuit voltage (V_{oc}), and current, voltage, and power at maximum power point (I_{mp}, V_{mp}, P_{mpp}, respectively).

Subsequently, the total power output produced in each grid square of location (s) is calculated. For this, the usable rooftop area $A_{PV(s)}$ is calculated according to Eq. (1), where $A_{rt(s)}$ is the total available rooftop area in the grid square of location (s), and f_u is the rooftop utilization factor. Then, the number of modules N_m that can be installed inside the corresponding usable rooftop area $A_{PV(s)}$ of the grid square of location (s) is calculated according to Eq. (2), where A_m is the area of one PV module.

$$A_{PV_{(s)}} = A_{rt_{(s)}} \cdot f_u \tag{1}$$

$$N_m = A_{PV_{(s)}} / A_m \tag{2}$$

The total power output $P_{total(s)}(t)$ produced in the grid square of location (s) at time (t) is calculated according to Eq. (3), where $P_{mpp(s)}$ is the hourly output power at the maximum power point from the SAPM model simulated using the meteorological data of location (s) at time (t), N_m is the number the PV modules, and the factor f_{loss} accounts for the system losses.

$$P_{total_{(s)}}(t) = N_m \cdot P_{mpp_{(s)}}(t) \cdot (1 - f_{loss}) \tag{3}$$

Note that the $P_{mpp(s)}$ is used for the calculation of the total power output to have a unique criterion of the performance of the modeled systems; however, under real operational conditions the power output may vary among PV systems.

The process described above is repeated for each grid square of each study area. Then, the resulting power output time series associated with the specific geographical coordinates of the grid square centroid are collected in a dataset and exported as NetCDF file.

The annual energy yield E_{annual} in each study area is calculated according to Eq. (4), where y equals 8760 h in a year and k represents the total number of grid squares inside the study area.

$$E_{annual} = \sum_{s=1}^{k} \sum_{t=0}^{y} P_{total_{(s)}}(t) \tag{4}$$

At the end of the process, one file for each study area is generated in such a way that the accumulated annual or monthly energy yield, hourly averages and other statistics can be calculated in Python. Additionally, the annual energy yield results are exported as raster layer to be visualized in QGIS. Figure 5 illustrates the input datasets used for the calculation and the technical potential output raster map.

4.3 Economic assessment

4.3.1 Levelized cost of electricity: The economic viability of solar PV technologies depends on the possibility of substituting an existing source of electricity with that from a PV system, which is commonly evaluated by comparing the levelized cost of electricity (LCOE) against the current electricity prices [9]. The LCOE expressed in [USD/kWh] is defined as the total cost (investment plus operational costs) of a power-generating asset over its lifetime divided by the total energy output of the asset over that lifetime [37], and calculated according to Eq. (5) [38].

$$\mathrm{LCOE} = \frac{\left(\mathrm{CAPEX} + \sum_{n=1}^{N} \frac{\mathrm{OPEX}}{(1+r)^n}\right) \cdot P_I}{\sum_{n=1}^{N} \frac{E_0 \cdot (1-D)^n}{(1+r)^n}} \tag{5}$$

where:

CAPEX: total initial investment (capital expenditures) [USD/kWp].

OPEX: annual operation and maintenance expenditures [USD/kWp].

P_I: total installed capacity [kWp].

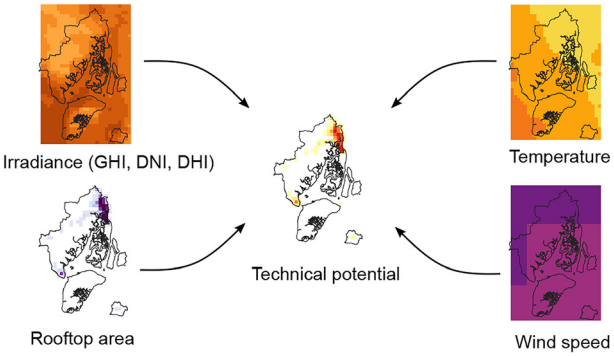

Figure 5: Illustration of the input datasets used for the technical rooftop PV potential assessment in Guayaquil.

E_0: initial annual energy yield [kWh].
r: discount rate [%].
D: system degradation rate [%].
n: year considered [–].
N: PV system lifetime [years].

As suggested in ref. [38], we calculate the LCOE under three financial scenarios (called low, medium and high), using different values for CAPEX, OPEX, and r, which are selected based on multiple literature sources summarized in Table 2. The reference values for CAPEX and discount rate for each scenario are selected based on recent studies on economic assessment of PV systems in Ecuador listed in Table B1 of Appendix B, while the reference values for OPEX are calculated as 1% of the investment costs, following the criterion used in refs. [39, 40], who assessed PV systems in Ecuador and Brazil, respectively. A linear degradation of 0.5% per year [9, 38] and a lifetime of 25 years [38] are assumed for the three scenarios.

4.3.2 Electricity tariffs in Ecuador: In Ecuador the electricity tariff regime depends on the geographical area and is designed in such a way that the electricity prices increase in steps according to the range of the monthly energy consumption [43]. The increase is slight for low monthly consumption, while it is exponential for consumption above 500 kWh/month [44]. This aspect is relevant since there is not a

Table 2: Input parameters for the economic assessment under three financial scenarios.

Input parameter	Units	Low	Medium	High	References
CAPEX	USD/kWp	1110	1433	1970	[11, 39, 41]
OPEX	USD/kWp	11.10	14.33	19.70	[39, 40]
Discount rate	%	7.00	8.68	10.71	[10, 39, 42]
Degradation rate	%	0.5	0.5	0.5	[9, 38]
Lifetime	Years	25	25	25	[38]

fixed reference price for determining the economic potential of rooftop PV, but rather a range. To simplify the analysis, we assume representative electricity tariffs for residential users in each study area, which are defined based on previous studies as described below.

For Quito and Guayaquil, we use the findings from ref. [44], who performed a clustering analysis of electricity consumption data from both cities in order to (i) classify customers according to consumption range and category (residential, commercial and industrial), and (ii) calculate the representative consumption per category. According to the results, almost 85% of consumers fall into the residential category with a consumption less than 500 kWh/month [44]. Further, the representative monthly consumption for this category was 145.21 kWh/month in Guayaquil, while in Quito was around 116 kWh/month [44]. Therefore, the representative electricity tariff of 8.3 USD cents/kWh is assumed for our analysis, which is the base tariff for the consumption range 101–150 kWh/month in these areas according to the regulated tariffs listed in ref. [43].

In the case of Cuenca and the Galapagos Islands, no similar studies were found in the literature. For this reason, the selection of the representative electricity tariff for these areas is based on the Ecuadorian electricity sector statistics of 2019 reported in ref. [45]. According to the statistics more than 98% of the consumers in both areas fall into the residential category, suggesting that typical monthly consumption could be similar to consumption in Guayaquil and Quito. Thus, the representative electricity tariff of 9.5 USD cents/kWh is assumed for our analysis in Cuenca and the Galapagos Islands, which corresponds to the base tariff for consumption range 101–150 kWh/month in those regions according to the regulated tariffs listed in ref. [43].

In addition to the cost of monthly energy consumption, the final electricity bill for residential users in Ecuador includes fees for commercialization and public lighting services [43]. Therefore, it is necessary to take into account these fees to analyze the economic viability of PV roof systems. Table 3 shows the total residential electricity tariffs assumed in this study, which are calculated based on the listed representative consumption and following the approach used in ref. [39]. Note that the calculated additional fees in USD cents/kWh are only an approximation, since in reality the commercialization and public lighting fees are paid monthly regardless of consumption. The final electricity bill may also include different subsidies [43], although these are not taken into account in this study.

4.4 Sensitivity analysis

A local sensitivity analysis is conducted to quantify the impact of the individual parameters for the calculation of the technical and economic assessment. The one-factor-at-a-time method is selected for this purpose, which consists in the variation of each variable within a defined range while keeping the others fixed and calculating the value of the parameter of interest [46]. Table 4 shows the sensitivity ranges for the input parameters involved in the annual energy yield and the LCOE selected based on the literature consulted.

First, the annual energy yield or LCOE is re-calculated varying the input parameter within the corresponding range. Then, a simple linear regression is performed to (i) model the relation between the dependent parameters of interest (energy yield or LCOE) and the changed input parameters (except for the azimuth angle), and (ii) obtain the correlation coefficients [47]. The fitted lines from the regression analysis are used to re-calculate the values of LCOE and energy yield by replacing the values of the input parameters. Finally, the results are expressed as a percentage of variation with respect to the base case values. In the case of the azimuth angle, the re-calculated annual energy yield is displayed in a polar plot for the different orientations relative to due north.

Table 3: Assumed representative residential electricity tariffs for each study area, which are calculated based on data from refs. [39, 43, 44].

Study area	Base tariff	Representative consumption	Commercialization fees		Public lighting fees		Total tariff
	[USD cents/kWh][a]	[kWh/month]	[USD/ consumer/ month]	[USD cents/ kWh]	[USD/ consumer/ month]	[USD cents/ kWh]	[USD cents/ kWh]
Quito	8.3	116.00[b]	1.414	1.22	1.50	1.29	10.81
Guayaquil	8.3	145.21[b]		0.97		1.03	10.31
Cuenca	9.5	125.50[c]		1.13		1.20	11.82
Galapagos Islands	9.5	125.50[c]		1.13		1.20	11.82

[a]Regulated electricity tariffs in 2019 for the corresponding representative monthly consumption in each study area. Source: ref. [43], [b]representative monthly consumption found in ref. [44], [c]average of the representative monthly consumption range (101–150 kWh/month).

Table 4: Sensitivity range for the input parameters involved in the calculation of energy yield and LCOE.

Input parameter	Units	Sensitivity range	Step	References
Utilization factor	–	0.3–0.6	0.05	[48, 49]
Tilt angle	Degrees	5–25[a]	1	[31, 50]
Azimuth angle	Degrees	0–360	22.5	[50]
System losses	–	0.1–0.3	0.01	[51, 52]
CAPEX	USD/kWp	750–2000	50	[10, 39]
OPEX	USD/kWp	5–30	1	[38]
Discount rate	%	4–10[b]	0.5	[10, 38]
Degradation rate	%	0.1–1.0[c]	0.1	[9, 38]
Lifetime	years	20–25	1	[39, 41]

[a]The lower limit tilt angle is set at 5°, which is the minimum angle recommended to avoid dirt accumulation on the PV modules [50], [b]the range for the discount rate is based on the more optimistic value from the European market [38] and the highest rate for the studies in Ecuador [10], [c]the degradation rate range is set from 0.1% to 1% taken as midpoint the typically rate of 0.5% considered in refs. [9, 38].

5 Results and discussion

5.1 Available rooftop area

The results of the geospatial assessment under the base case assumptions reveal a total available rooftop area of 143.88 km^2 over all the study areas. Table 5 summaries the results and compares the available rooftop area with the population statistics. Guayaquil and Quito have large rooftop areas (61.11 and 69.00 km^2, respectively), while Galapagos have the highest value in terms of rooftop area per capita (41.66 m^2 per

Table 5: Summary of the estimated available rooftop area in each study area and comparison with population statistics from 2010. Source: Own calculations and statistical data from ref. [19].

Study area	Number of polygons	Available rooftop area [km^2]	Rooftop area per inhabitant [m^2 per capita]	Share in the total estimated rooftop area [%]
Quito	862,650	61.11	25.99	42.47
Guayaquil	456,053	69.00	30.81	47.96
Cuenca	77,939	12.72	25.16	8.84
Galapagos Islands	–	1.05	41.66	0.73
Total	**1 396,642**	**143.88**	**28.09**	**100**

inhabitant). Note, however, that the calculations for Galapagos are not based on the digital cadastral maps (see Table 1).

Figure 6 displays the spatial distribution of the available rooftop area under the base case input parameters in each study area. In Quito, the roofed area is highly concentrated (~89%) between latitudes 0.5 °S and 0 °N where the urban parishes are located. Lower available rooftop area is seen in the east and north, where rural land is predominant. In Guayaquil, the total available rooftop area is 69 km^2 considering a factor of 0.65 as the maximum building coverage ratio, since the digital map comprises cadastral parcels (see Section 3.1). The highest concentration of roofed area lies on the northeast between longitude 80 °W to 79.8 °W and latitudes 2 °S to 2.3 °S. In Cuenca, the total area is 12.72 km^2 of which ~7.8 km^2 (61%) belongs to the urban zone, where more than half of the roofed area is placed at latitude 2.94 °S between longitudes 79 °W and 78.8 °W. In the rural parishes, the rooftop area is 7.56 km^2 calculated from the cadastral parcel map, which is reduced to 4.91 km^2 considering a factor of 0.65 as the maximum building coverage ratio. In the Galapagos Islands, the total rooftop area is 1.05 km^2, assuming a 30% of rooftop area occupation in the urban zones. Santa Cruz Island (located between latitudes 0.5 °S and 0.75 °S) shows the largest rooftop area (0.5 km^2), which is distributed between the parishes Puerto Ayora, Bellavista and Santa Rosa with 0.38 km^2, 0.052 km^2 and 0.055 km^2, respectively. The rooftop area for San Cristobal Island is 0.33 km^2, from which 0.03 km^2 belongs to Puerto Velasco and approximately 0.30 km^2 to Puerto Baquerizo Moreno. Isabela Island has 0.21 km^2 of rooftop area accumulated in Puerto Villamil.

5.2 Technical assessment results

Table 6 provides a summary of the estimated technical rooftop PV potential under the base case input parameters and assuming that 100% of the usable rooftop area were developed. Quito and Guayaquil have the highest technical potential with an annual energy yield over 7000 GWh/a. This high potential is related to the large rooftop area

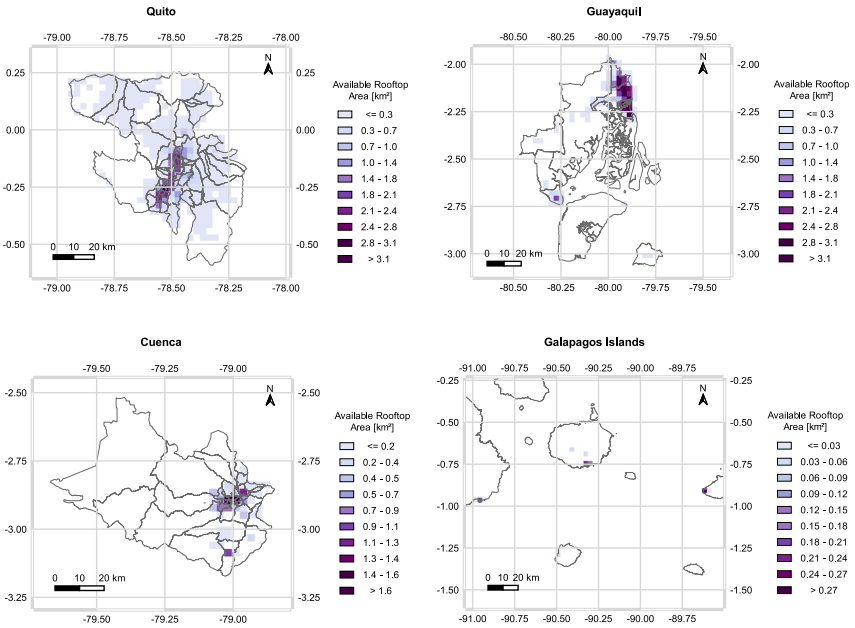

Figure 6: Spatial distribution of the available rooftop area under the base case assumptions in each study area with a grid resolution of 3 × 3 km.
Source: Own calculations, data retrieved from refs. [22–25].

available in those study areas. In contrast, Cuenca and the Galapagos Islands have lower potential, with an annual energy yield equal to 1475 and 135 GWh/a, respectively. Nevertheless, the results in terms of generation per rooftop area show that Galapagos have the highest technical PV potential, which is to be expected since the irradiation level on the islands is higher than on the other continental areas. The specific yield values shown in Table 6 also reflect the large potential in Galapagos (1458.62 kWh/kWp), closely followed by the potential in Quito (1452.98 kWh/kWp).

The comparison between the estimated rooftop PV annual energy yield and the electricity consumption in 2019 reported in ref. [45] shows that the rooftop PV generation surpasses the annual consumption in all study areas (Table 6). This is a remarkable result that implies that the 54.77% of the estimated technical potential could cover the annual electricity consumption in these areas.

The spatial distribution of the rooftop PV annual energy yield under the base case assumptions for each study area is shown in Figure 7, where it is evident that the potential is centered in areas with the highest building concentration, as shown in the geospatial assessment results in Section 5.1.

A more detailed look at the estimated annual energy yield under the base case assumptions aggregated by parishes in Quito, Guayaquil and Cuenca is shown in

Table 6: Summary of the estimated technical rooftop PV potential in each study area under the base case assumptions. Source: Own calculations, irradiance data from NSRDB and consumption statistics in 2019 from ref. [45].

Study area	Annual mean daily total GHI [Wh/m^2/day]	Energy yield per rooftop area[a] [kWh/m^2/a]	Estimated installed capacity[a] [MWp]	Specific energy yield[b] [kWh/kWp]	Annual energy yield[c] [GWh/a]	Annual electricity consumption in 2019[d] [GWh/a]	Technical potential needed to cover annual consumption[e] [%]
Quito	4302.11	128.48	5403.74	1452.98	7851.51	3375.50	42.99
Guayaquil	4574.57	108.43	6101.62	1226.20	7481.82	5025.84	67.17
Cuenca	4562.23	115.93	1125.11	1311.02	1475.04	821.97	55.73
Galapagos Islands	5645.79	128.97	92.55	1458.62	135.00	55.89	41.40
				Total	**16,943.37**	**9279.20**	**54.77**

[a]Results under the base case assumptions for the technical assessment, [b]ratio between total annual energy yield if 100% of the usable rooftop area were developed and the estimated installed capacity under the base case assumptions, [c]expected electricity output if 100% of the usable rooftop area were developed, [d]total annual electricity consumption in 2019 from all consumption groups (residential, commercial, industrial, public lighting and others) reported in ref. [45], [e]based on electricity consumption statistics in 2019 reported in ref. [45] and assuming the use of the total estimated technical potential.

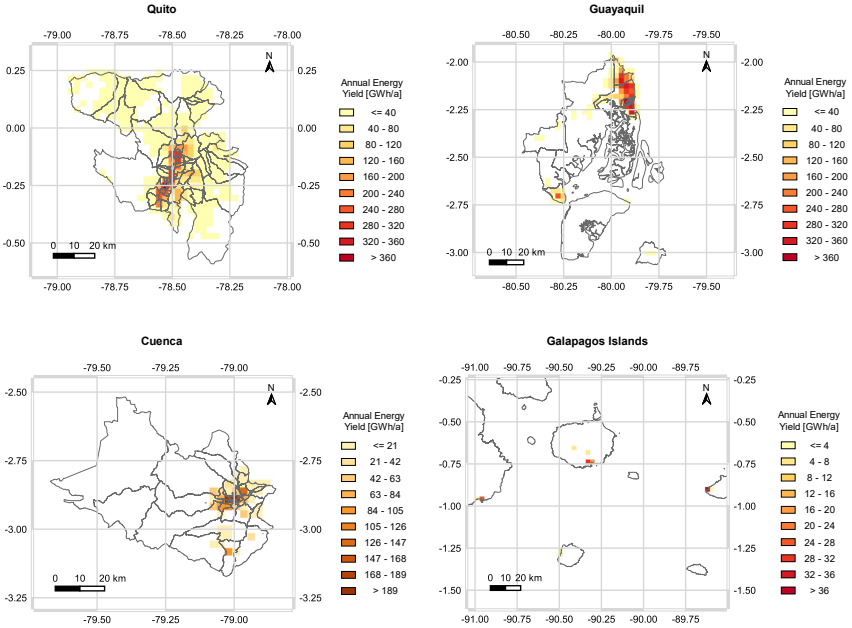

Figure 7: Spatial distribution of rooftop PV annual energy yield under the base case assumptions with a grid resolution of 3 × 3 km.

Figure 8. Additionally, the comparison between the expected annual energy yield by parishes and the electricity consumption in 2019 disaggregated by consumption type is shown in Figures C.1–4 in Appendix C. From these figures, it can be seen that the parishes Calderon and Conocoto in Quito, which are densely populated peri-urban parishes, have the highest annual yield (570.95 and 413.09 GWh/a, respectively). In Cuenca, Yanuncay that is the biggest and most populated urban parish shows the highest annual yield (147.51 GWh/a), while Ricaurte that is a rural parish takes the second place (110.16 GWh/a). In Guayaquil, Tarqui, which is the biggest and most populated urban parish, shows the highest annual yield (2554.09 GWh/a). In Galapagos, Puerto Ayora and Puerto Baquerizo Moreno account for the highest annual yield (47.96 and 41.38 GWh/a, respectively).

What stands out in Figures C.1–4 is that the estimated rooftop PV potential surpasses the annual electricity consumption of almost all parishes of the study areas. The exceptions are the parishes Iñaquito that has a high commercial consumption in Quito, Hermano Miguel that has the highest industrial consumption in Cuenca, and Ximena that has the highest industrial and commercial consumption in Guayaquil, according to the electricity consumption statistics in 2019 reported in ref. [45].

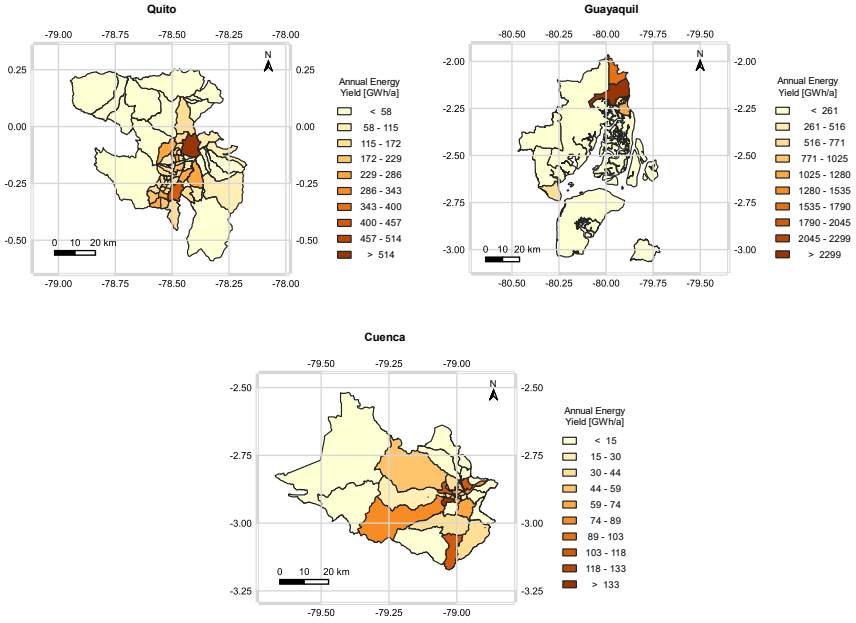

Figure 8: Estimated annual energy yield under the base case assumptions aggregated by parishes in Quito, Guayaquil and Cuenca.

5.2.1 Comparison between monthly rooftop PV generation and electricity consumption

The comparison between the monthly estimated energy yield and the recorded electricity consumption in 2019 is shown in Figure 9. From this figure, it is evident that the estimated PV generation exceeds the electricity consumption throughout the year in all study areas. It can also be seen that the monthly consumption is relatively stable (especially in Quito and Cuenca). In contrast, the PV generation shows an intra-annual variability, which is related to the spatio-temporal variability of the solar resource previously investigated in ref. [26].

In Quito, the estimated average monthly PV production is 654.29 GWh with high values between June and August (787.11 GWh max.) and low values from November to February (542.76 GWh min.). In contrast, the average monthly consumption is 281.29 GWh with a variation no greater than 3% throughout the year. The low intra-annual variability of energy consumption is related to the low seasonal oscillation of ambient temperature in Quito, which consequently reduces the need of electric-based heating or cooling systems for interior spaces. The peak consumption is reached in November (286.11 GWh), while the lowest consumption occurs in March (273.14 GWh).

The estimated PV production in Guayaquil shows a bimodal pattern (Figure 9) with two peaks occurring in March–May and August–September (698.61 GWh max.) and a

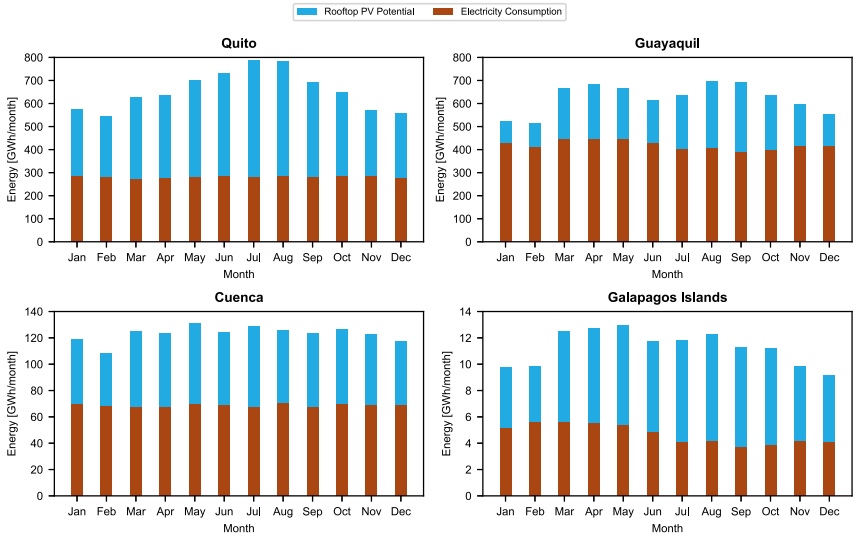

Figure 9: Comparison of estimated energy yield under base case assumptions in each study area against the monthly electricity consumption during 2019 from all consumption groups (residential, commercial, industrial, public lighting and others).
Source: Own calculations and consumption statistics in 2019 from ref. [45].

minimum in February (516.43 GWh). In contrast, the electricity consumption in Guayaquil shows a unimodal pattern with a peak in May (446.94 GWh) and minimum in September (387.10 GWh). The seasonal behavior of the energy consumption seems to be correlated to the increased use of air conditioners driven by the rise of temperature and relative humidity [53]. The estimated average monthly PV production is 623.49 GWh, while the average consumption is 418.82 GWh.

Figure 9 also shows that both the estimated PV production and electricity consumption in Cuenca display low intra-annual variability. The estimated average monthly PV production is 121.49 GWh, with the highest production in May (130.72 GWh) and the lowest in February (108.50 GWh). In contrast, the average consumption is 68.50 GWh and the intra-annual variability of energy consumption is low. Similar to Quito, the ambient temperature in Cuenca is stable and comfortable throughout the year, which reduces the need of electric-based heating or cooling systems for interior spaces [31]. The peak consumption occurs in August (70.43 GWh), while the lowest consumption occurs in July (66.89 GWh).

In Galapagos, the highest production is reached in May (12.92 GWh), dropping from November to February and reaching a minimum in December (9.17 GWh). In contrast, the electricity consumption shows a peak in March (5.6 GWh) and a minimum in September (3.69 GWh). The increase of consumption from December to May corresponds to the peak tourist season [54]. The estimated average monthly PV production is 11.11 GWh, while the consumption records an average of 4.66 GWh.

5.2.2 Comparison between hourly rooftop PV generation and electricity demand profiles

Examining the time series of the expected rooftop PV generation against the electricity demand at an hourly scale is necessary to understand the consequences for the local energy balance, since increased PV penetration can lead to instability of the grid and considerably escalate the storage and system back-up requirements [55]. In order to provide an overview of this comparison, we use a typical hourly demand profile from residential and commercial users in Quito taken from ref. [39].

The comparison shows that PV generation does not match the demand periods for residential users (Figure 10a). The demand curve shows a small peak around 7 am and another of higher magnitude at 7 pm, while PV generation reaches its highest production between 10 am and 2 pm, when residential electricity demand is low. In the case of commercial users (Figure 10b), the first demand peak occurs between 9 and 11 am, which corresponds to the maximum PV generation hours; however, the second peak occurs from 5 to 7 pm when PV output is decreasing. This comparison suggests that the estimated rooftop PV technical potential could not be completely exploited without the use of storage systems or on-grid connections to feed the excess rooftop PV energy into the grid. Nevertheless, it should be noted that a more detailed analysis of production-demand imbalances is needed, using hourly demand time series for a whole year instead of typical profiles. In this way, the seasonal variations, which are seen especially in Guayaquil and Galapagos (Figure 9), can be captured to better understand the imbalances between the rooftop PV production and the demand in each study area. The lack of open-access data on electricity demand at higher than monthly temporal resolution, however, hinders such assessments.

5.3 Economic assessment results

Figure 11 shows the comparison of the calculated LCOE under the three different financial scenarios with the assumptions listed in Table 2. It is important to highlight that these results are based on the assumption that 100% of the estimated technical potential under the base case input parameters is exploited. The lowest LCOE values under all scenarios are seen in Quito and the Galapagos Islands, while Guayaquil has the highest values. When comparing the results by scenarios, the LCOE increases as the financial condition are more unfavorable, meaning that the highest values are obtained under the high scenario.

A comparison between the estimated LCOE against the representative residential electricity tariffs under the different scenarios is shown in Figure 11. The results suggest that PV generation is cost-competitive in all study areas under the low scenario, which considers optimistic initial investment costs and a low discount rate. In contrast, the assumptions of the medium scenario are more realistic, since they are based on current

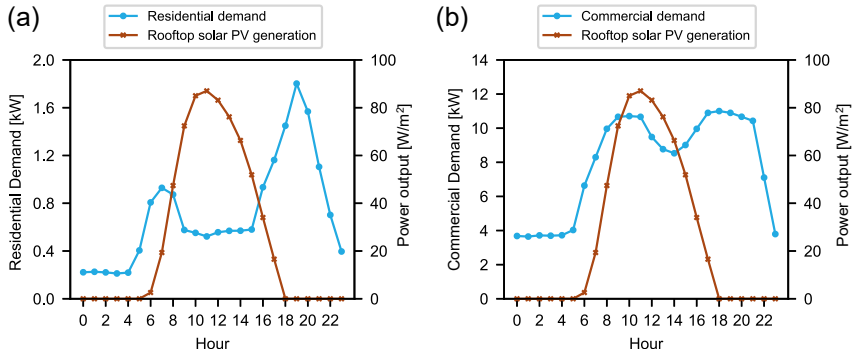

Figure 10: Comparison of estimated hourly average power output per rooftop area against typical hourly demand profile in Quito for (a) residential users (average monthly consumption of 500 kWh) and (b) commercial users (contracted power 11 kW).
Source: Own calculations and consumption data from ref. [39].

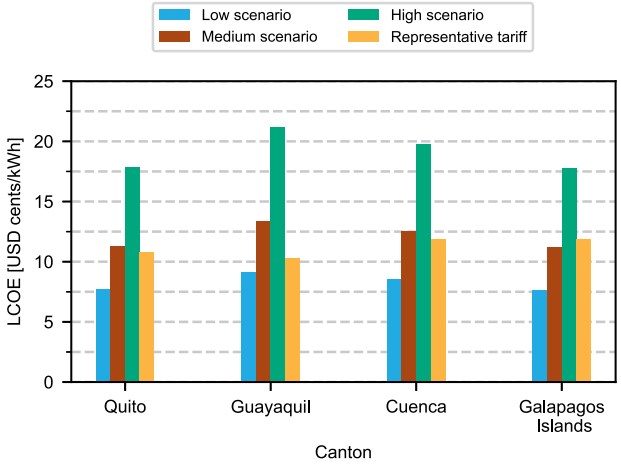

Figure 11: Comparison of estimated LCOE per study area under three financial scenarios if 100% of the usable rooftop area under the base case assumptions were exploited.

financial conditions. However, the results suggest that under this scenario rooftop PV is cost-competitive only in Galapagos. This is an interesting outcome that suggest that despite showing the lowest technical potential rooftop PV generation in Galapagos would be cost-competitive, which may be explained by the fact that the irradiation levels are higher on the islands as compared to the other areas (Table 6). The LCOE values calculated under the high scenario suggest that PV generation is not cost-competitive in any of the study areas, since the generation would cost between 65 and

105% more compared to the representative residential tariffs. Nevertheless, it must be kept in mind that this scenario assumes the highest expenditures and discount rates.

The resulting LCOE calculated in this study are aligned to previous solar PV assessment in Ecuador. For instance, in ref. [11] the estimated LCOE was 12 USD cents/kWh for PV solar generation in Cuenca (12.62 USD cents under the medium scenario). Also, in ref. [56] the estimated LCOE for PV solar generation in Ecuador was calculated between 11.21 and 13.34 USD cents/kWh with a tendency to be more cost-competitive comparing to the tariffs in the future. In this respect, according to the projections from the Inter-American Development Bank, investment cost for PV projects are expected to decrease progressively in Ecuador (950 USD/kWp in 2023) [57], which would be reflected in lower LCOE values for rooftop PV as well.

In this work we compare only the calculated LCOE against tariffs for residential users since the scope of this study is to assess the rooftop PV potential at a city level using representative tariffs. However, the analysis of single systems with a specific power capacity and demand requirements could provide further insights about the rooftop PV economic feasibility for industrial and commercial users. For instance, Benalcázar et al. [39] assessed the competitiveness to integrate small-scale PV systems (5 and 10 kWp) for self-consumption of commercial users in Quito. The authors concluded that the implementation of PV systems for commercial users is economically feasible, representing reductions of around 12% and 25% compared to monthly electricity bills from the utility company. Further, the current regulation framework for self-consumption using distributed energy systems under a monthly net energy balance scheme [5] is expected to provide economic incentives for users and to support the penetration of solar PV rooftop technology in Ecuador.

5.4 Sensitivity analysis results

5.4.1 Sensitivity analysis for technical parameters

The variability of the estimated energy yield with respect to changes of ±20% in the input parameters is shown in Figure 12, where similar change patterns are seen in each study area. The largest deviations on the energy yield with respect to the base case are caused by the variations of the utilization factor f_u. This is because f_u impacts the calculation of the usable rooftop area $A_{PV(s)}$, which at the same time determines the number of PV modules that can be installed (see Eqs (1) and (2)). Therefore, a higher usable rooftop area leads to a higher generation capacity.

Changes in the f_{loss} factor have a greater impact on the energy yield compared to those due to the tilt angle, but less compared to variations due to the f_u factor (Figure 12). The estimated annual yield for Quito and Guayaquil deviates up to ±0.1 TWh/a per each 1% of variation in the f_{loss} factor. For Cuenca and Galapagos this deviation is equivalent to ±0.01 and ±0.001 TWh/a, respectively. As expected, the

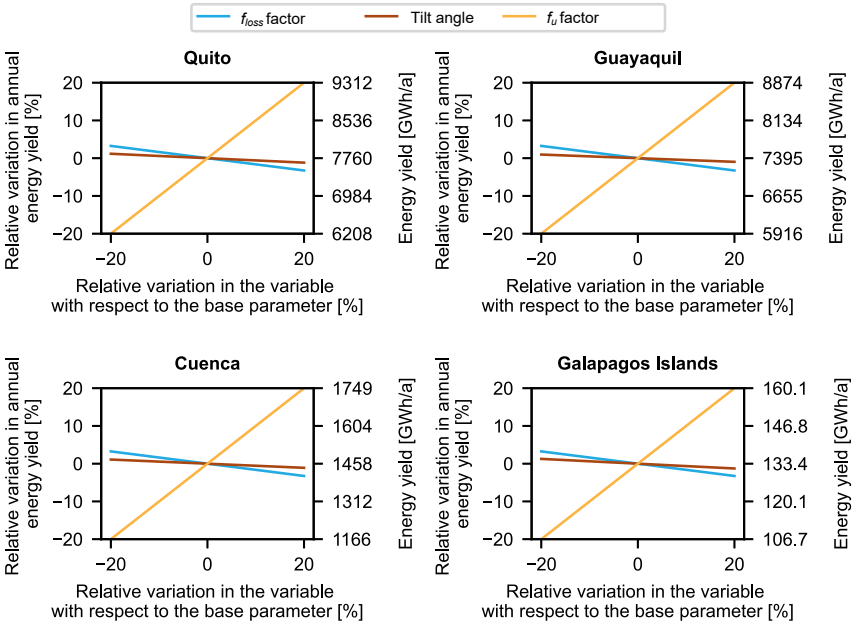

Figure 12: Variability of the estimated energy yield in each study area with respect to changes of ±20% in the input parameters.

relation between energy yield and f_{loss} is inverse, i.e., as f_{loss} increases the energy yield decreases. However, note that the analysis of the sensitivity of f_{loss} shows aggregated results, since this factor represents losses due to several causes (e.g., shading, dust, wiring, etc.). Nevertheless, this approach has been performed in previous assessments at a regional or national level (e.g., ref. [9, 58]). An alternative method for disaggregating losses due to shading could be, for instance, to model shadows on building roofs for each pixel at a given sun position (see e.g., ref. [27]). Such an approach was beyond the scope of the present study; however, it could be applied in Quito and the urban area of Cuenca, since the digital cadastral maps characterize the building footprint in these areas.

From Figure 12 it is also evident that variation in the tilt angle within the selected range has the lowest impact on the energy yield calculation for all study areas. The maximum deviation of the energy yield is around ±1.5% for changes of ±20% in the base case tilt angle (20°). This minor effect is explained by the fact that sun's declination varies little over the equator and there is no strong seasonality as observed in places at lower or higher latitudes. This finding is consistent with that of Serrano-Guerrero et al. [50], who found that the optimal flat surfaces inclination to maximize solar irradiation capture is between 9° and 16°. Similarly, Barragán-Escandón et al. [59] found that losses become significant when tilt angles are close to 30°.

The variation of the annual energy yield with respect to the azimuth and tilt angle is shown in Figure 13, where it can be seen that the impact from this parameter is different among the study areas. In Quito, the orientation towards east (90 ± 22.5° relative to due north) with 20° inclination leads to higher potential. In Guayaquil, flat roofs or those oriented between 0° and 45° relative to due north with 10° inclination show higher potentials. In Cuenca and Galapagos, flat roofs or those oriented between 45° and 90° relative to due north with 10° inclination show higher potentials. In the case of Quito, the resulting east-facing optimal orientation can be explained by comparing the DNI average hourly values throughout the year (see Figure D.1 in Appendix D), in which a clear trend of high DNI values in the morning and low values in the afternoon is seen, suggesting that PV generation decreases in the afternoon due to more cloudy conditions, therefore favoring the east-facing orientation. These findings are contrary to theoretical recommendations that suggest the orientation of modules towards north for countries located in the southern hemisphere [60]. However, our findings are consistent with those of Serrano-Guerrero et al. [50], who determined the optimal orientation and inclination of modules for solar energy applications using a modeling approach with data from meteorological stations in Cuenca and typical meteorological years datasets for other cities in Ecuador (including Quito and Guayaquil).

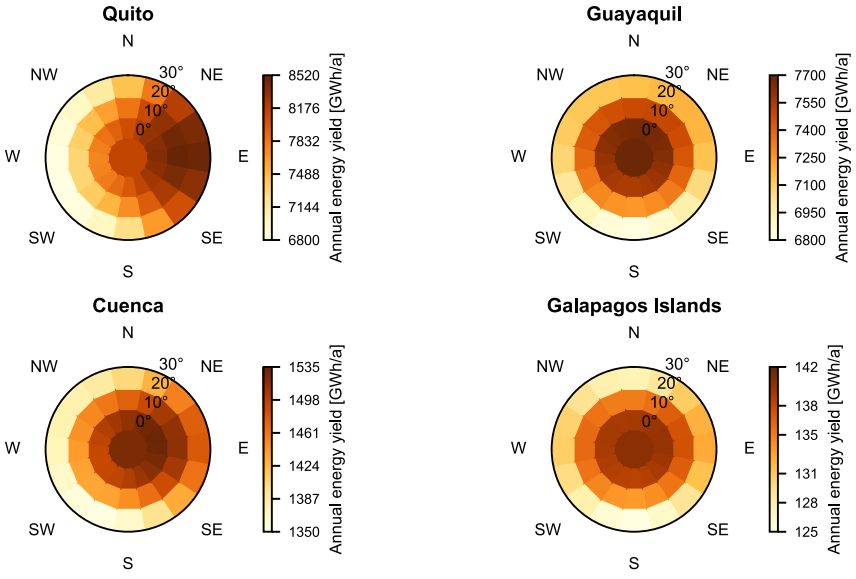

Figure 13: Polar plot of annual energy yield for different roof tilt and orientation in each study area. The radius indicates the tilt angle, while the polar angle refers to the orientation.

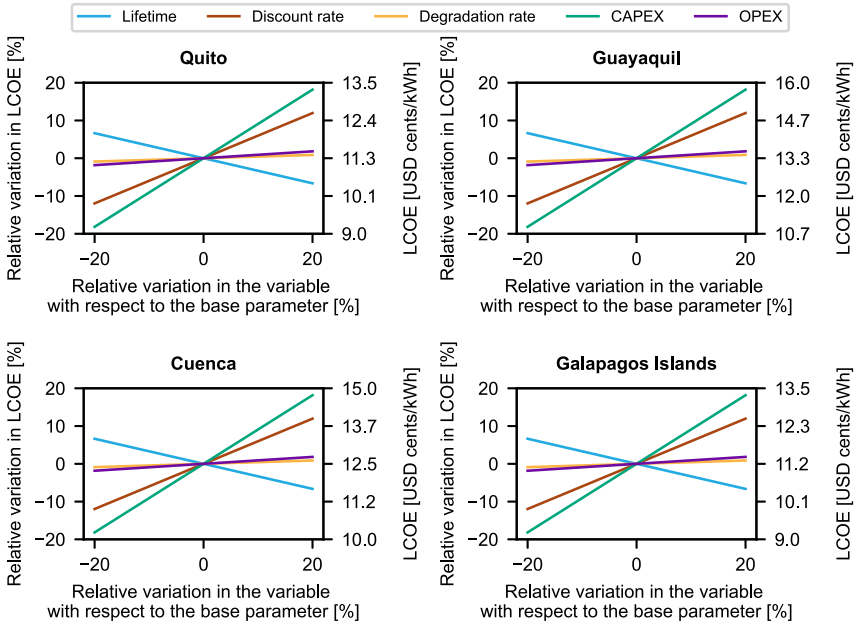

Figure 14: Results of the sensitivity analysis for economic parameters in each study area.

5.4.2 Sensitivity analysis for economic parameters

The results of the sensitivity analysis for the economic parameters shown in Figure 14 reveal that the most sensitive parameters for the LCOE calculation are CAPEX and discount rate *r*. Variations in the CAPEX produce a deviation of almost the same order in the LCOE, i.e., a variation of ±100 USD/kWh in the CAPEX represents a deviation up to ±0.9 USD cents/kWh in the LCOE with respect to the initial estimates. The OPEX has a lower effect as compared to the CAPEX, since a change of ±20% in the OPEX produces a deviation lower than ±2% in the LCOE. In solar PV systems, the initial investment costs represent the greatest portion of the PV lifecycle costs, therefore it is expected that the variations in CAPEX have more effects on the LCOE than the OPEX [38].

Figure 14 also indicates a strong influence of the discount rate in the LCOE calculation. A variation of ±20% in the base case discount rate causes a deviation around ±12% in the LCOE with respect to the initial estimates. This effect stems from the mathematical formulation of the LCOE (see Eq. (5)). The degradation rate has less impact in the PV generation costs as a variation of ±20% produces a deviation lower than 1% in the initial LCOE estimates. The changes in this parameter affects the PV module performance, i.e., an increment on the degradation leads to higher performance losses and consequently to a reduction on the energy yield [38]. Nevertheless, the typical values considered for this rate are low (around 0.5% annual), thus its impact is lower compared to the other parameters.

The lifetime shows a reciprocal relation with the LCOE, meaning that longer lifetime decreases generation costs. The results show that a variation of ±20% in the base case lifetime can produce a deviation close to ±7% in the LCOE respect to the initial estimates (Figure 14). This suggests that an extension of 1 year in the expected lifetime of PV modules can reduce on 0.17 USD cents/kWh the generation costs. This is explained by the fact that the changes in the lifetime of the PV systems affect the amortization time of the investment costs [38].

6 Conclusions

The present study provides a comprehensive assessment of the potential of rooftop solar PV in high populated cities of Ecuador's mainland and the Galapagos Islands, using gridded satellite-derived solar resource data and readily available GIS datasets. Based on the assumptions explained in this work, the results show that Quito, Guayaquil and Cuenca have a total rooftop PV potential of 16.81 ± 3.36 TWh/a, while the inhabited islands of Galapagos have a potential of 135.00 ± 27.00 GWh/a. These results suggest that the estimated rooftop PV potential could cover the electricity consumption recorded in 2019, even if only half of it is exploited. Due to the high levels of radiation and low seasonal variability seen in the study areas, the solar resource could be exploited throughout the year. Nevertheless, the comparison between the estimated hourly PV generation and the typical hourly demand profile for residential and commercial users indicates that the peak demand occurs outside the period of maximum PV power output. Therefore, to exploit the estimated technical potential, it is necessary to use storage systems or on-grid connections to feed surplus into the grid.

The results from the financial scenario analysis reveal that rooftop PV technology is cost-competitive in all study areas only under the low scenario, which considers optimistic initial investment costs and a low discount rate. However, under the medium and high scenarios the PV generation cost estimated in terms of LCOE is higher than the reference electricity tariffs for residential users. This is mainly due to subsidies for electricity generation in Ecuador, which are reflected in lower electricity prices for end-users. Nevertheless, the current Ecuadorian regulatory framework of distributed generation for self-consumption includes a net energy metering scheme, which provides an economic incentive to promote rooftop PV installations in residential, commercial and industrial sectors. Besides, according to the sensitivity analysis, the capital expenditures and discount rate are the most influential parameters for the LCOE; therefore, the establishment of strategies to create cost-competitive conditions, such as tax exemptions to reduce investment costs, could foster the end-user's attractiveness of implementing rooftop PV systems.

The insights gained from this work will be of interest for local authorities and other decision makers to design policies and financing strategies to increase the penetration of rooftop PV and displace fossil fuel power generation. The described methodology can be used to assess the potential in other Ecuadorian regions and thereby support a sustainable energy transition in the country. Further research might explore in more detail the technical potential of the urban zones with high rooftop density identified in this study. For instance, the use of high-resolution building data and shading evaluation methods would help in reducing the uncertainties in the calculations.

Acknowledgments: This manuscript is based on the master's thesis by Leonard Ramos, conceptualized and supervised by Mariela Tapia. We thank the High-Performance Computing Team from the University of Oldenburg for their computing facilities. The first author dedicates this work in memory of Prof. Dr. Stefan Gößling-Reisemann.
Author contributions: **Mariela Tapia:** Conceptualization, methodology, formal analysis, writing – original draft, writing – review and editing. **Leonard Ramos:** Methodology, software, visualization, formal analysis, validation, writing – original draft. **Detlev Heinemann:** writing – review and editing. **Edwin Zondervan:** Writing – review and editing.
Research funding: This research did not receive any specific grant from funding agencies in the public, commercial, or not-for-profit sectors.
Conflict of interest statement: The authors declare no conflict of interest.

Appendix A

Table A1: Main input parameters for the SAPM model of the selected PV module (SunPower SPR 220 BLK-U). Source: ref. [61].

Parameter	Unit	Value	Parameter	Unit	Value
Vintage	–	2008	I_{x_0}	–	5.4651
Material	–	Mono-c-Si	I_{xx_0}	–	3.7619
Area	m^2	1.244	α_{Isc}	–	0.000179
Cells in series	–	72	α_{Imp}	–	−0.000435
I_{so0}	A	5.468	β_{Voc_0}	–	−0.145022
V_{oc0}	V	47.832	β_{Vmp_0}	–	−0.1492
I_{mp0}	A	5.086	$m_{\beta Voc_0}$	–	0
V_{mp0}	V	39.335	$m_{\beta Vmp_0}$	–	0

Appendix B

Table B1: Overview of main parameters for the economic assessment of rooftop PV systems used in recent studies regarding PV assessment in different regions of Ecuador.

Author, Year	Region	Capacity [kWp]	Type	CAPEX [USD/kWp]	OPEX [USD/kWp]	Discount rate [%]	Lifetime [years]	Reference
Benalcazar et al., 2020	Quito	3	Single system	1970	0.5–1% of	7.00	25	[39]
		5		1840	CAPEX			
		10		1780				
Bermeo et al., 2021	Azogues	62.4	Single system	1110	–	7.15	20	[41]
Barragán et al., 2019	Cuenca	314,270	Aggregated at a city level	1433	17.2	10.00	25	[11]
Dávila and vallejo, 2019	Quito	557,100	Aggregated at a city level	750[a]	–	10.71	25	[10]
Trejo, 2021	Ibarra	7.68	Single system	3042[b]	0	8.68	25	[42]

[a]This value was not considered for the selection because according to ref. [10] it represents an hypothetical scenario,[b]this value was not considered for the selection because the calculations uses prices of flexible PV modules [42], which are more expensive compared to the modules used in our study.

Appendix C

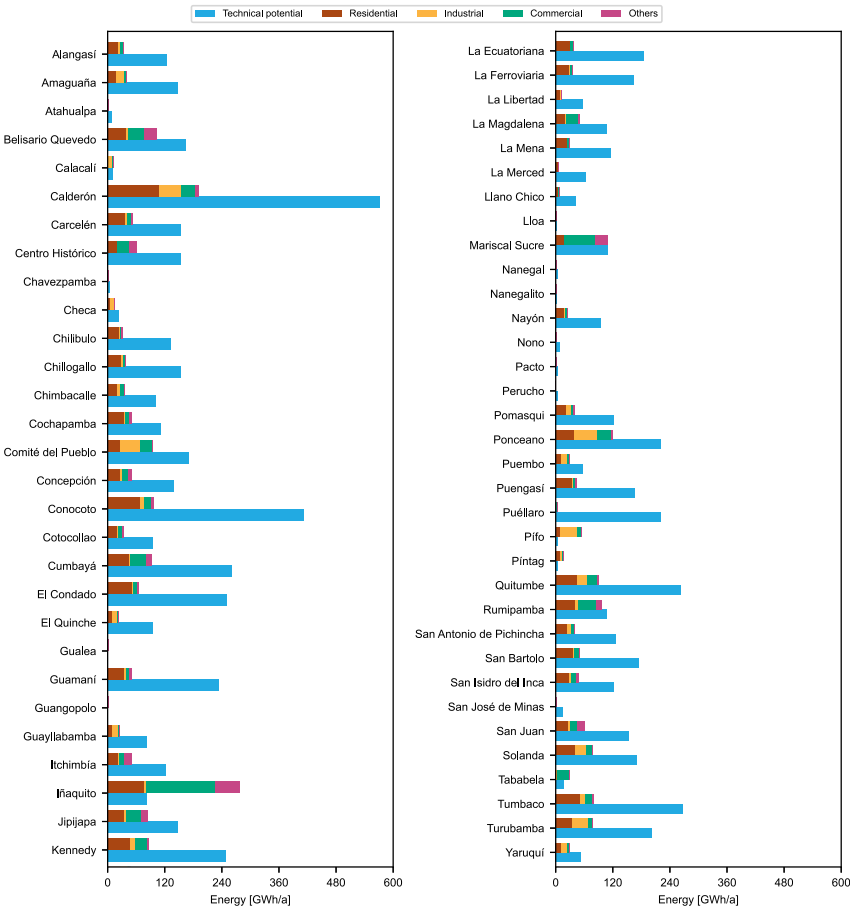

Figure C.1: Comparison of the estimated annual energy yield under the base case assumptions and electricity consumption in urban and rural parishes of Quito disaggregated by consumption groups (residential, commercial, industrial and others).
Source: Own calculations and consumption statistics in 2019 taken from ref. [45].

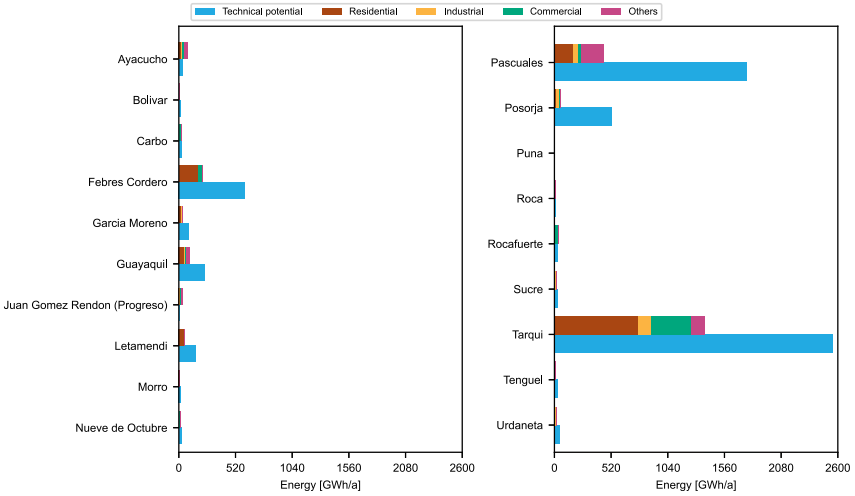

Figure C.2: Comparison of the estimated annual energy yield under the base case assumptions and electricity consumption in urban and rural parishes of Guayaquil disaggregated by consumption groups (residential, commercial, industrial and others).
Source: Own calculations and consumption statistics in 2019 taken from ref. [45].

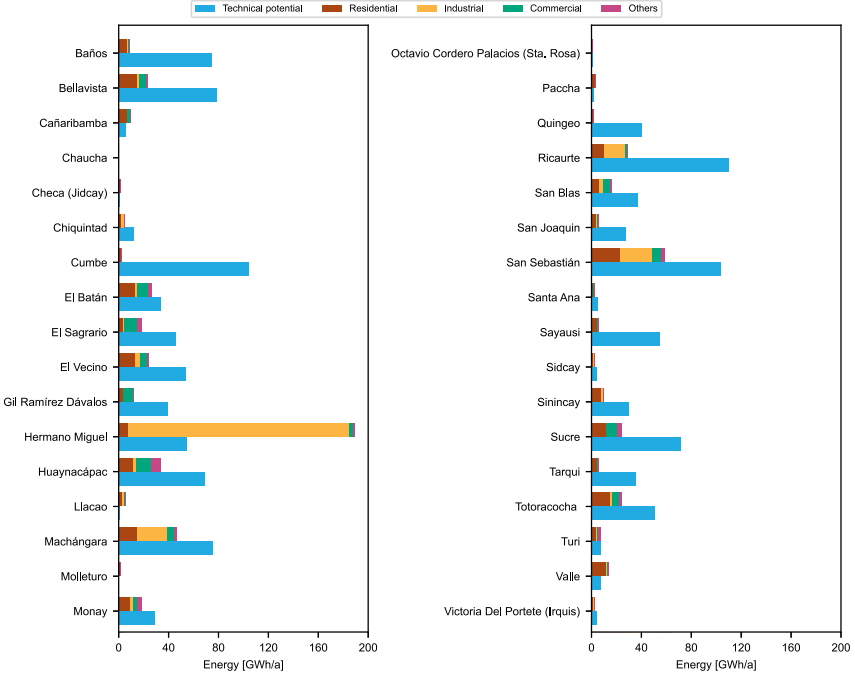

Figure C.3: Comparison of the estimated annual energy yield under the base case assumptions and electricity consumption in urban and rural parishes of Cuenca disaggregated by consumption groups (residential, commercial, industrial and others).
Source: Own calculations and consumption statistics in 2019 taken from ref. [45].

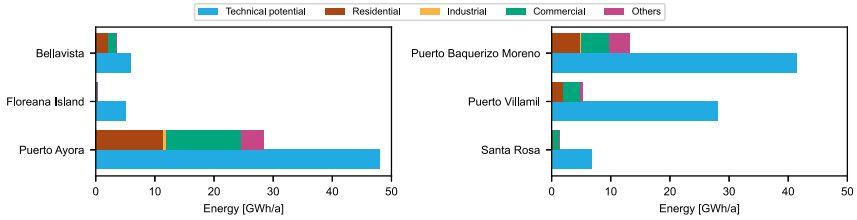

Figure C.4: Comparison of the estimated annual energy yield under the base case assumptions and electricity consumption in parishes of the Galapagos Islands disaggregated by consumption groups (residential, commercial, industrial and others).
Source: Own calculations and consumption statistics in 2019 taken from ref. [45].

Appendix D

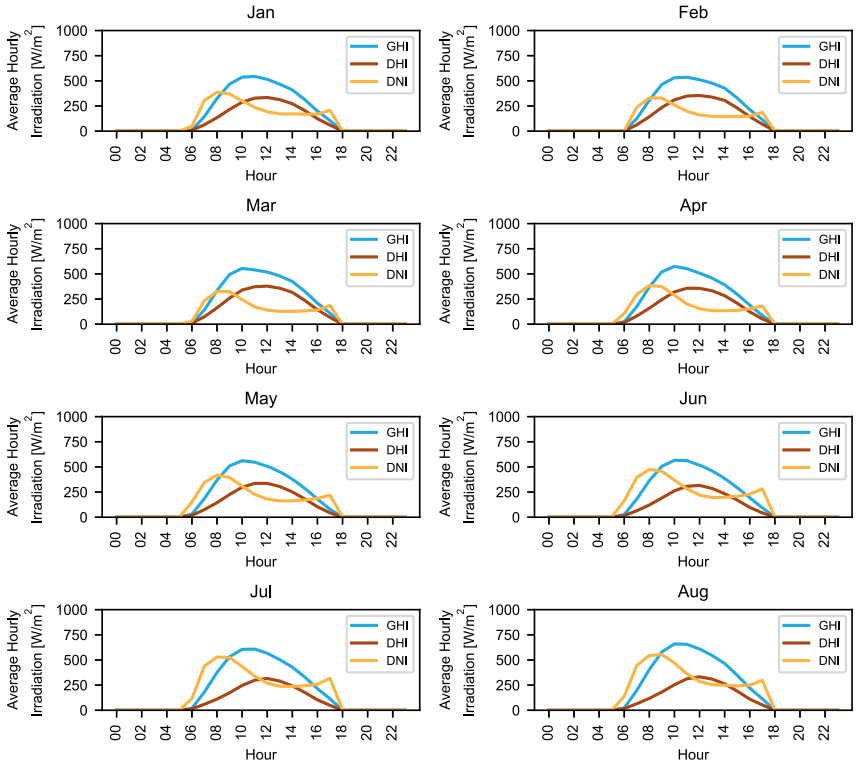

Figure D.1: Long-term hourly averages of solar irradiance components from 1998 to 2018 in Quito. Data retrieved from the NSRDB.

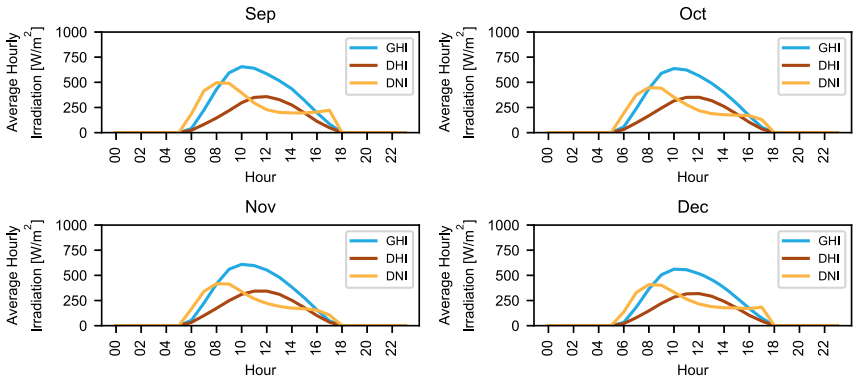

Figure D.1: Continued.

References

1. IRENA. Rise of renewables in cities: energy solutions for the urban future; 2020. Available from: https://www.irena.org/-/media/Files/IRENA/Agency/Publication/2020/Oct/IRENA_Renewables_in_cities_2020.pdf.
2. Jaeger-Waldau A. PV status report 2018. Luxembourg (Luxembourg): Publications Office of the European Union; 2018.
3. Ordoñez F, Vaca-Revelo D, Lopez-Villada J. Assessment of the solar resource in andean regions by comparison between satellite estimation and ground measurements: study case of Ecuador. J Sustain Dev 2019;12:62–75.
4. ARCERNNR. Estadística anual y multianual del sector eléctrico ecuatoriano 2020; 2021. Available from: https://www.controlrecursosyenergia.gob.ec/estadisticas-del-sector-electrico-ecuatoriano-buscar/ [Accessed 16 Feb 2022].
5. ARCERNNR, Resolucion Nro. ARCERNNR-013/2021; 2021. Available from: https://www.controlrecursosyenergia.gob.ec/wp-content/uploads/downloads/2021/06/res_nro__arcernnr-013-2021.pdf [Accessed 13 Feb 2022].
6. Salazar S, Arcos H. Análisis técnico y económico de la implementación del net metering para diferentes tipos de consumidores de electricidad en el ecuador. Rev Técnica "Energía" 2021;18:86–94.
7. Byrne J, Taminiau J, Kurdgelashvili L, Kim KN. A review of the solar city concept and methods to assess rooftop solar electric potential, with an illustrative application to the city of Seoul. Renew Sustain Energy Rev 2015;41:830–44.
8. Schallenberg-Rodríguez J. Photovoltaic techno-economical potential on roofs in regions and islands: the case of the Canary Islands. Methodological review and methodology proposal. Renew Sustain Energy Rev 2013;20:219–39.
9. Bódis K, Kougias I, Jäger-Waldau A, Taylor N, Szabó S. A high-resolution geospatial assessment of the rooftop solar photovoltaic potential in the European union. Renew Sustain Energy Rev 2019;114:109309.
10. Dávila R, Vallejo D. Evaluación del potencial técnico y económico de la tecnología solar fotovoltaica para la microgeneración eléctrica en el sector residencial del distrito metropolitano de Quito. Escuela Politécnica Nacional; 2019. Available from: https://bibdigital.epn.edu.ec/handle/15000/786%0Ahttps://bibdigital.epn.edu.ec/bitstream/15000/786/1/CD-1222.pdf.

11. Barragán-Escandón A, Zalamea-León E, Terrados-Cepeda J. Incidence of photovoltaics in cities based on indicators of occupancy and urban sustainability. Energies 2019;12:1–26.
12. Tian A, Zünd D, Bettencourt LMA. Estimating rooftop solar potential in urban environments: a generalized approach and assessment of the Galápagos Islands. Front Sustain Cities 2021;3:1–11.
13. Sengupta M, Xie Y, Lopez A, Habte A, Maclaurin G, Shelby J. The national solar radiation data base (NSRDB). Renew Sustain Energy Rev 2018;89:51–60.
14. NREL, System Advisor Model (SAM); 2022. Available from: https://sam.nrel.gov/ [Accessed 21 Feb 2022].
15. Solargis, World BankGroup. Global solar atlas; 2020. Available from: https://globalsolaratlas.info/download/ecuador [Accessed 21 Feb 2022].
16. Noboa A. El modelo de organización territorial del Ecuador con énfasis en la actividad normativa de los gobiernos locales. Quito: Universidad Andina Simón Bolivar; 2013:1–85 pp. http://hdl.handle.net/10644/3752 [Accessed 21 Feb 2022].
17. Lemos M. Historia de la organización territorial en el Ecuador. Guayaquil: Universidad de Guayaquil; 2019.
18. Instituto Geográfico Militar, Geoportal IGM; 2021. Available from: http://www.geoportaligm.gob.ec [Accessed 26 Jan 2022].
19. Instituto Nacional de Estadística y Censos (INEC), Censo de Población y Vivienda; 2010. Available from: http://www.ecuadorencifras.gob.ec/censo-de-poblacion-y-vivienda/ [Accessed 28 Apr 2021].
20. GAD Municipal de Guayaquil, Gaceta Oficial No. 18; 2020. Available from: https://www.guayaquil.gob.ec/wp-content/uploads/Documentos/Gacetas/Periodo 2019-2023/Gaceta 18.pdf [Accessed 31 Jan 2022].
21. GAD Municipal Cuenca. Anexos PUGS – actualizado a Septiembre 2021; 2021: 165 p. Available from: http://www.cuenca.gob.ec/sites/default/files/planificacion/Anexos PUGS-actualizado a septiembre 2021.pdf [Accessed 31 Jan 2022].
22. Secretaría General de Planificación, Geoportal del Municipio del Distrito Metropolitano de Quito; 2021. Available from: http://geoportal.quito.gob.ec/smiq/ [Accessed 6 May 2021].
23. GAD Municipal de Guayaquil, Geoportal del GAD Municipal de Guayaquil; 2021. Available from: https://geoportal-guayaquil.opendata.arcgis.com [Accessed 6 May 2021].
24. GAD Municipal Cuenca, Geoportal Cuenca; 2021. Available from: https://ide.cuenca.gob.ec/geoportal-web [Accessed 5 May 2021].
25. Consejo de Gobierno del Régimen Especial, Geoportal Galápagos; 2021. Available from: http://geoportal.gobiernogalapagos.gob.ec [Accessed 5 May 2021].
26. Tapia M, Heinemann D, Ballari D, Zondervan E. Spatio-temporal characterization of long-term solar resource using spatial functional data analysis: understanding the variability and complementarity of global horizontal irradiance in Ecuador. Renew Energy 2022;189:1176–93.
27. Walch A, Castello R, Mohajeri N, Scartezzini JL. Big data mining for the estimation of hourly rooftop photovoltaic potential and its uncertainty. Appl Energy 2020;262:114404.
28. QGIS Association, QGIS Geographic Information System; 2022. Available from http://www.qgis.org [Accessed 13 Jun 2022].
29. Lawhead J. QGIS python programming cookbook. Birmingham: Packt Publishing Ltd; 2015.
30. Holmgren WF, Hansen CW, Mikofski MA. Pvlib python: a python package for modeling solar energy systems. J Open Source Softw 2018;3:884.
31. Zalamea-León E, Mena-Campos J, Barragán-Escandón A, Parra-González D, Méndez-Santos P. Urban photovoltaic potential of inclined roofing for buildings in heritage centers in equatorial areas. J Green Build 2018;13:45–69.
32. Dobos A. PVWatts version 5 manual; 2014, Technical Report NREL/TP-6A20-62641.

33. King DL, Boyson WE, Kratochvil JA. Photovoltaic array performance model; 2004, Tech. Rep. SAND2004–3535.
34. Morocho I, Ríos K. Estudio técnico para incorporar generación distribuida fotovoltaica en el sector residencial del cantón Cuenca. Universidad Politécnica Salesiana Sede Cuenca; 2015. Available from: https://dspace.ups.edu.ec/handle/123456789/7516.
35. pvlib, pvlib python; 2022. Available from: https://pvlib-python.readthedocs.io/en/stable/index.html [Accessed 6 Feb 2022].
36. Hay JE, Davies JA. Calculation of the solar radiation incident on a inclined surface. In: Hay JE, Won TK, editors. Proc. 1st can. sol. radiat. data work. Downsview, Canada: Canadian Atmospheric Environment Service; 1980:59–72 pp.
37. Gómez-Navarro T, Brazzini T, Alfonso-Solar D, Vargas-Salgado C. Analysis of the potential for PV rooftop prosumer production: technical, economic and environmental assessment for the city of Valencia (Spain). Renew Energy 2021;174:372–81.
38. Tjengdrawira C, Richter M, Theologitis IT. Best practice guidelines for PV cost calculation; 2016. Available from: http://www.solarbankability.org/fileadmin/sites/www/files/documents/20161213_649997_Best_Practice_Guidelines_for_PV_Cost_Calculation_20161213.pdf.
39. Benalcázar P, Lara J, Samper M. Distributed photovoltaic generation in Ecuador: economic analysis and incentives mechanisms. IEEE Lat Am Trans 2020;18:564–72.
40. Dávi GA, Caamaño-Martín E, Rüther R, Solano J. Energy performance evaluation of a net plus-energy residential building with grid-connected photovoltaic system in Brazil. Energy Build 2016; 120:19–29.
41. Bermeo I, Matute L, Barragán-Escandón E, Serrano-Guerrero X, Zalamea-León E. Technical and economic feasibility study of a solar plant on a commercial surface in Azogues, Ecuador. Renew Energy Power Qual J 2021;19:177–83.
42. Trejo R. Estudio de factibilidad técnica económica para la implementación de un sistema de generación fotovoltaica en el edificio de la facultad de ingeniería en ciencias aplicadas. Ibarra: Universidad Técnica del Norte; 2021. http://repositorio.utn.edu.ec/handle/123456789/11213 [Accessed 21 Feb 2022].
43. ARCONEL. Pliego tarifario para las empresas eléctricas de distribución codificado; 2019. Available from: https://www.regulacionelectrica.gob.ec/wp-content/uploads/downloads/2019/07/P-Tarifario-SPEE-2019_Codif.pdf.
44. Salazar G. Análisis técnico y económico de la implementación del net metering para diferentes tipos de consumidores de electricidad en el Ecuador. Quito: Escuela Politécnica Nacional; 2020: 1–119 pp. http://bibdigital.epn.edu.ec/handle/15000/20937 [Accessed 21 Feb 2022].
45. ARCERNNR. Reportes de información estadística del sector eléctrico. Facturación clientes regulados 2019; 2021. Available from: http://reportes.controlrecursosyenergia.gob.ec [Accessed 8 Feb 2022].
46. Cacuci DG, Ionescu-Bujor M. A comparative review of sensitivity and uncertainty analysis of large-scale systems—II: statistical methods. Nucl Sci Eng 2004;147:204–17.
47. Walpole R, Myers R, Myers S, Ye K. Probability and statistics for engineering and science, 9th ed Boston: Pearson; 2012.
48. Mainzer K, Fath K, Mckenna R, Stengel J, Fichtner W, Schultmann F. A high-resolution determination of the technical potential for residential-roof-mounted photovoltaic systems in Germany. Sol Energy 2014;105:715–31.
49. Melius J, Margolis R, Ong S. Estimating rooftop suitability for PV: a review of methods, patents, and validation techniques; 2013, Technical Report NREL/TP-6A20-60593.
50. Serrano-Guerrero X, Cantos E, Feijoo JJ, Barragán-Escandón A, Clairand JM. Optimal tilt and orientation angles in fixed flat surfaces to maximize the capture of solar insolation: a case study in Ecuador. Appl Sci 2021;11:1–4.

51. Maghami MR, Hizam H, Gomes C, Radzi MA, Rezadad MI, Hajighorbani S. Power loss due to soiling on solar panel: a review. Renew Sustain Energy Rev 2016;59:1307–16.
52. Mainzer K, Killinger S, McKenna R, Fichtner W. Assessment of rooftop photovoltaic potentials at the urban level using publicly available geodata and image recognition techniques. Sol Energy 2017;155:561–73.
53. Litardo J, Hidalgo-Leon R, MacIas J, Delgado K, Soriano G. Estimating energy consumption and conservation measures for ESPOL Campus main building model using EnergyPlus. In: 2019 IEEE 39th cent. am. panama conv. CONCAPAN 2019. Novem; 2019.
54. Eras-Almeida AA, Egido-Aguilera MA, Blechinger P, Berendes S, Caamaño E, García-Alcalde E. Decarbonizing the Galapagos Islands: techno-economic perspectives for the hybrid renewable mini-grid Baltra-Santa Cruz. Sustain 2020;12:1–47.
55. Ramirez Camargo L, Zink R, Dorner W, Stoeglehner G. Spatio-temporal modeling of roof-top photovoltaic panels for improved technical potential assessment and electricity peak load offsetting at the municipal scale. Comput Environ Urban Syst 2015;52:58–69.
56. Muñoz-Vizhñay JP, Rojas-Moncayo MV, Barreto-Calle CR. Incentivo a la generación distribuida en el Ecuador. Ingenius 2018;19:60–8.
57. García de Fonseca L., Parikh M., and Manghani R. 2019. *Evolución futura de costos de las energías renovables y almacenamiento en América Latina* (Juan Paredes (ed.)). Banco Interamericano de Desarrollo División de Energía. https://doi.org/10.18235/0002101.
58. Khuong PM, McKenna R, Fichtner W. A cost-effective and transferable methodology for rooftop PV potential assessment in developing countries. Energies 2020;13:1–46.
59. Barragán-Escandón E, Zalamea-León E, Terrados-Cepeda J, Vanegas-Peralta PF. Energy self-supply estimation in intermediate cities. Renew Sustain Energy Rev 2020;129:1–25.
60. Jacobson MZ, Jadhav V. World estimates of PV optimal tilt angles and ratios of sunlight incident upon tilted and tracked PV panels relative to horizontal panels. Sol Energy 2018;169:55–66.
61. NREL. SAM/deploy/libraries/; 2021. Available from: https://github.com/NREL/SAM/tree/develop/deploy/libraries [Accessed 22 Feb 2022].